applied sciences

MDPI

Article

Experimental Assessment of Correlative Approaches for the Prediction of Leakage Flow through Labyrinth Seals

Niccolò Castelli [1], Tommaso Bacci [1], Alessio Picchi [1,*], Lorenzo Winchler [2] and Bruno Facchini [1]

[1] Department of Industrial Engineering (DIEF), University of Florence, 50139 Firenze, Italy; niccolo.castelli@unifi.it (N.C.); tommaso.bacci@unifi.it (T.B.); bruno.facchini@unifi.it (B.F.)
[2] Baker Hughes—Nuovo Pignone Tecnologie, 50127 Firenze, Italy; lorenzo.winchler@bakerhughes.com
* Correspondence: alessio.picchi@unifi.it

Abstract: Simple analytical models can be employed to estimate the leakage mass flow rate from labyrinth seals, resulting in a quick procedure, well suited for the early design process. Different formulas were proposed by many authors during the past decades and most of them employ a carry-over factor and a flow coefficient to predict the mass flow rate across the clearance area. The present work aims to compare the analytical prediction with the results of an experimental campaign. The experimental results were retrieved from a dedicated test rig for both a straight-through and a stepped labyrinth seal. Hence, for each seal, the effect of the clearance size, the Reynolds number and the pressure ratio has been investigated. Starting from the experimental required inputs, six different correlations are considered, with both direct and indirect methods. The results are shown as a function of pressure ratio and clearance gap. Despite some differences in the comparison, and most of the used correlation underestimate the measured mass flow rate, some general trends and guidelines can be highlighted.

Keywords: labyrinth seals; analytical methods; experimental; leakage; secondary flows; correlation

Citation: Castelli, N.; Bacci, T.; Picchi, A.; Winchler, L.; Facchini, B. Experimental Assessment of Correlative Approaches for the Prediction of Leakage Flow through Labyrinth Seals. *Appl. Sci.* **2023**, *13*, 6863. https://doi.org/10.3390/app13126863

Academic Editor: Antonio Ficarella

Received: 15 May 2023
Revised: 1 June 2023
Accepted: 4 June 2023
Published: 6 June 2023

1. Introduction

One of the most important issues in turbomachinery design is the proper description, prediction and control of secondary flows. The prime example of this aspect is leakage flows. Efficient sealing systems must be employed to mitigate the total amount of air passing through the rotating and stationary components of the engine, since flow instabilities and, in general, efficiency reduction can occur if clearances and mass flow rates are too large. On the other hand, very small gaps can result in stator and rotor rubbing. Having a proper gap between stationary and rotating parts is core to ensuring the correct operating of the whole machine and to improve its life [1]. Labyrinth seals are currently the most common sealing methods used in the turbomachinery field since they have been introduced at the beginning of the previous century. The flow inside a labyrinth seal undergoes a series of consecutive constrictions and cavities as it is bounded by two relatively moving components, namely the teeth and the seal land. According to [2], two mechanisms occur inside a labyrinth; first, the flow accelerates as it approaches the clearance gap and a part of the pressure energy is converted into kinetic energy; then, part of the kinetic energy is dissipated in the cavity downstream of the constriction due to multiple phenomena, such as uncontrolled expansion, turbulence and viscous effects. The process repeats for each tooth of the labyrinth so that the flow resistance increases and hence, the control increases over the leakage flow rate. During the past decades, many parameters have been investigated in order to understand their influence on the labyrinth performance, such as pressure ratio [3,4], Reynolds number [3], clearance gap [4,5], tooth shape [6,7] and rotational speed [8,9]. It is clear that such a complexity should require some suitable CFD tools or a dedicated test campaign in order to evaluate both the flow field inside the seal

cavities and the leakage flow rate. However, correlations can be employed to estimate the mass flow through the constrictions during the very first stages of the design process to obtain some useful information for the labyrinth dimensioning. Such a procedure saves a lot of time since it relies on some simple equations.

In 1908, Martin first studied the labyrinth glands as a series of discrete throttling passages acting similar to a series of orifices and proposed his well-known formula. Since then, many efforts have been made to develop new equations to carefully predict the leakage mass flow. Although each equation tries to model the same flow phenomena in different ways and with different levels of detail, all the existing models involve two parameters: a flow coefficient and a carry-over factor. The first one accounts for the effective amount of air which flows across the tip clearance due to the interaction with the boundary layer near the tooth tip; on the other hand, the carry-over factor considers the fact that the air inside the cavity is not completely brought to rest and hence, some kinetic energy is carried over to the following constriction. In general, direct and indirect approaches have been developed. The direct correlations employ lumped quantities which accounts for the behavior of the whole seal, without attempting to resolve the pressure drop between the different teeth. As a result, only one equation with a single calculation step is solved. On the contrary, the indirect approaches model the effects of each tooth by means of continuity equation across a single cavity, which allows us to determine the pressure distribution downstream each tooth.

It is clear, therefore, that the reliability of the adopted correlative approach is crucial to the accuracy of the preliminary design phase, thus influencing, in turn, the speed and accuracy of the following detailed design. Therefore, the validation of different correlative approach, using detailed experimental data, is a relevant aspect of labyrinth seals research. An attempt was made, among others, by Szymanski et al. [6] for straight-through labyrinth seals. In most of the studies dealing with this topic, the comparison is made as a function of the pressure ratio across the seal, while the impact other aspect, such as the Reynolds number, on the correlations performance are not often considered. The present work aims to compare and benchmark different correlations available in the literature with the results of an in-house experimental campaign, extending the analysis to both straight-through and stepped seals and assessing the impact of both pressure ratio and Reynolds number. For this purpose, different analytical models were considered, both direct and indirect. In the following section, the authors describe the equation they employed during the comparative analysis; then, the experimental test rig is described and the results are given as a function of seal pressure ratio, Reynolds number and tip clearance size. The precise impact of this last parameter on the correlations accuracy is also often overlooked by the works dealing with this validation. This paper also attempts to fill this void, showing that the reliability of several correlations is highly dependent on the value of this parameter.

2. Analytical Models

In this section, a brief description of the applied analytical models is given. As already mentioned before, the authors distinguish among direct and indirect models according to how the seal is outlined. Most of the presented formulas have been developed for straight-through labyrinth seals, but they can be extended to stepped seals under certain assumptions. It is worth highlighting that many models are available in the literature but only some of them have been selected for the present work. Most of the approaches, whose results are shown in this work, shares theory and formulas with several other correlations, which only differ for the choice of some parameters. Since the resulting differences between correlations falling in the same family are generally very limited, some of them are not shown, even if they were implemented and evaluated, without the content losing generality. This is specified in the following section. Due to the large number of geometrical parameters that must be considered in this description, the readers may refer to Figure 1, where the parameters nomenclature is illustrated; this nomenclature is the same throughout the whole paper. Finally, in order to summarize all the employed methods and

to provide a comprehensive glimpse of the involved parameters, Table 1 is given at the end of Section 2.

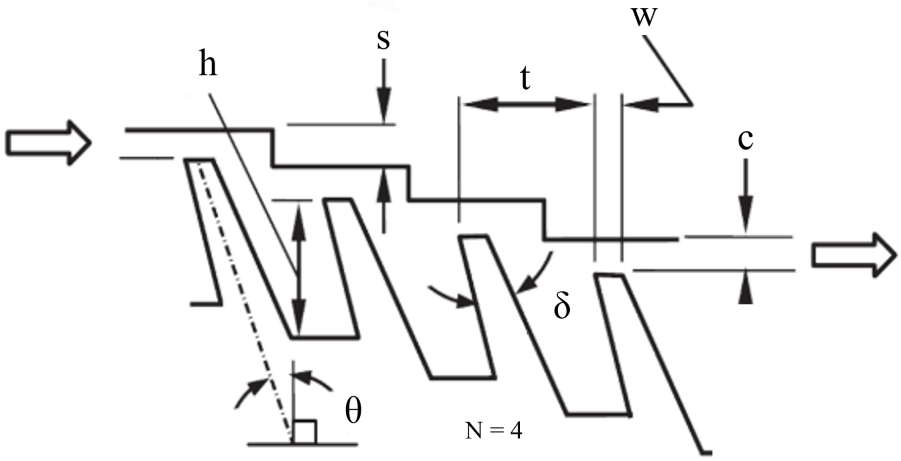

Figure 1. A 2D sketch of the experimentally tested stepped labyrinth seal. The main geometrical parameters are highlighted.

2.1. Direct Models

Before providing details on how researchers developed their equations, Martin's formula is given. Traditionally, this model was the first ever proposed. At the beginning of the previous century, Martin stated that each seal passage could be treated as a single sharp-edged orifice. His theory is based on three assumptions: (a) the process is isothermal, i.e., the inlet total temperature is the same for each teeth, (b) the velocities are everywhere subsonic and (c) all the kinetic energy is converted into heat inside the seal cavity and hence, no carry-over factor is included. Under these hypotheses, the leakage mass flow rate can be calculated as:

$$\dot{m} = K \cdot A \cdot \frac{p_{0,in}}{\sqrt{RT_{0,in}}} \cdot \sqrt{\frac{1 - (\frac{p_{s,N}}{p_{0,in}})^2}{N - \ln \frac{p_{s,N}}{p_{0,in}}}} \tag{1}$$

where A is the geometrical tip clearance area, $p_{0,in}$ is the total pressure upstream the first tooth, $T_{0,in}$ is the total temperature upstream the first tooth, $p_{s,N}$ is the static pressure downstream the last tooth and N is the number of labyrinth teeth. In the end, K is the flow coefficient of an annular orifice which can be experimentally derived as a function of the Reynolds number and the ratio between the tip width of the tooth and the clearance size (w/c). The need of a K value has been first explained by Egli [10] and is based on the idea that the actual area value A_j that should be used is lower than the geometrical area A and higher than the vena contracta one A_m (see Figure 2). The exact value corresponds to a section somewhere near the minimum one where the pressure in the air jet is equal to the cavity pressure. Since the position of this section is unknown, an empirical flow coefficient is employed to overcome this issue and fix the geometrical area value. The radicand term is often referred to as β and so it is described in the following for this treatment.

2.1.1. Hodkinson Equation

The Hodkinson model comes from the method developed by Egli in [10]. Thus, in order to provide a proper explanation of the current method, Egli's model is now illustrated. It is worth highlighting that it was numerically implemented and applied to the available experimental data but the results are not shown in the following since it is very similar to the more general Hodkinson equation.

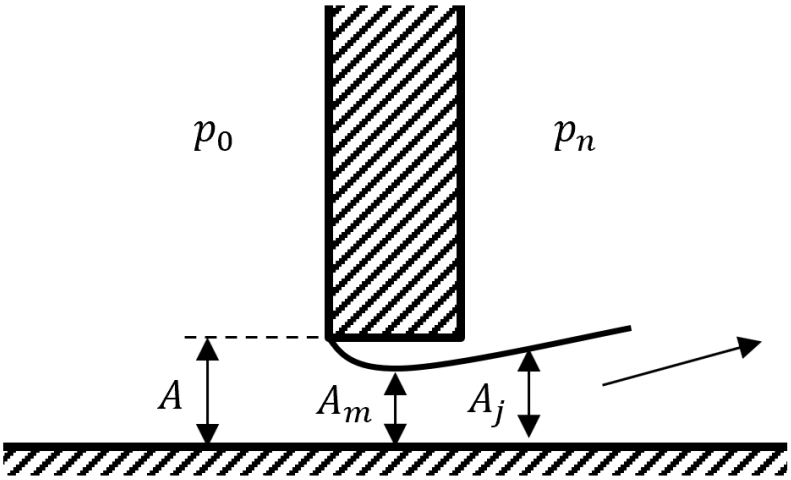

Figure 2. Uncontrolled expansion downstream a single sharp-edged orifice.

Egli derived his model directly from Martin's one with an empirical value for the flow coefficient. However, he added the carry-over factor (μ), since the shape of a straight-through labyrinth seal allows a considerable percentage of kinetic energy to be carried from one cavity into the next one. Hence, Equation (1) becomes:

$$\dot{m} = \mu \cdot K \cdot A \cdot \frac{p_{0,in}}{\sqrt{RT_{0,in}}} \cdot \sqrt{\frac{1 - (\frac{p_{s,N}}{p_{0,in}})^2}{N - \ln \frac{p_{s,N}}{p_{0,in}}}} \tag{2}$$

In addition, Egli stated that, actually, the flow coefficient can be directly related to the percentage of kinetic energy carried through each tooth and hence, to μ itself. Thus, K is assumed to be constant ($K = 0.65$) and the variation of leakage is accounted for by varying only μ. Egli obtained some empirical curves for labyrinths with a different number of teeth, showing that the kinetic energy carried over rises as the spacing between the teeth or the clearance gap increases. Starting from Egli's remarks, Hodkinson performed a series of dedicated experimental tests in order to retrieve a semi-empirical formula of the carry-over factor, defined as:

$$\mu = \sqrt{\frac{1}{1 - \left(\frac{N-1}{N}\right) \cdot \left(\frac{c/t}{c/t+0.02}\right)}} \tag{3}$$

Hodkinson developed this equation assuming that the jet downstream each tooth expands conically inside the cavity at a small angle from the fin tip [11]. The carry-over is clearly a function of the clearance-to-pitch ratio (c/t) and, for a fixed number of sealing points N, it increases as c/t increases. However, for a very large value of clearance, μ does not become infinity, but a constant asymptotic value is reached at approximately $\sqrt{N}$.

2.1.2. Vermes Equation

Vermes model for leakage mass flow in a labyrinth is probably the most famous one [2]. Following the same Martin's approach, Vermes suggested retrieving the flow coefficient K as a function of w/c and the flow Reynolds number, from some experimental data provided by Bell et al. [12]. Furthermore, a new formulation of the carry-over factor based on the boundary layer theory was proposed. It depends on geometrical features of the labyrinth, but not on the number of teeth, and is given by:

$$\mu = \sqrt{\frac{1}{1-\alpha}} \quad \text{with} \quad \alpha = \frac{8.52}{\frac{t-w}{c} + 7.23} \tag{4}$$

Although the number of teeth is not directly specified in Equation (4), it can be applied if N ranges from 3 to 34, as stated by [2].

2.1.3. Zimmermann Equation

Zimmermann also developed a correlation method based on Martin's formula [13]. He suggested a modified version of Hodkinson's carry-over multiplying μ by a correction factor μ_c, which describes more accurately the effect of the number of teeth and defined as:

$$\mu_c = \sqrt{\frac{N}{N-1}} \tag{5}$$

On the other hand, the flow coefficient can be retrieved from some experimental plots as a function of both the clearance-to-tooth width ratio (c/w) and the flow Reynolds number. In particular, if a straight-through labyrinth is considered, Zimmermann collected a series of data retrieved from both literature and industry, providing a K dependence on flow Reynolds number, while he suggested employing the values proposed by Snow et al. [14] for stepped labyrinth seals, where the flow coefficient depends on the overall pressure ratio PR. In addition, Zimmermann provided many other correction factors in order to properly estimate the effects of other geometrical features on the flow coefficient, such as grooves, honeycombs and tip radiusing. However, these features are neglected in the present work since they do not affect the tested labyrinth seals.

2.2. Indirect Models

Unlike the previous methods, where the bulk parameter β accounting for the overall pressure ratio across the seal is used, indirect models do not employ any bulk parameters, but they solve the one-dimensional continuity equation for each cavity. Hence, the mass flow leakage across the i-th constriction can be calculated by means of the following equation [15]:

$$\dot{m}_i = \mu_i \cdot K_i \cdot A \cdot \sqrt{\frac{p_i^2 - p_{i+1}^2}{R \cdot T_{0,in}}} \tag{6}$$

Since the leakage from a cavity to the next one stays constant, it is possible to recast Equation (6) by imposing $\dot{m}_1 = \dot{m}_2 = ... = \dot{m}_N = \dot{m}$. Thus, according to the number N of sealing points, a system of N equations and N variables (m, p_2, p_3, ..., p_{N-1}) can be written and solved through iterative methods; $p_1 = p_{0,in}$ and $p_N = p_{s,N}$ are known terms as inlet/outlet pressures across the seal. In this way, both the leakage mass flow and the pressure distribution across the labyrinth can be retrieved.

2.2.1. Neumann Equation

Neumann developed his model starting from the empirical flow equation presented by Childs in [16]. In particular, he adopted a flow coefficient defined by the Chaplygin formula (Gurevich, 1966 [17]) as:

$$K_i = \frac{\pi}{\pi + 2 - 5 \cdot \varphi_i + 2 \cdot \varphi_i^2} \quad \text{with} \quad \varphi_i = \left(\frac{p_i}{p_{i+1}}\right)^{\frac{\gamma-1}{\gamma}} - 1 \tag{7}$$

Whereas the direct models employ a unique value of flow coefficient for the entire labyrinth, this formulation allows us to obtain a different value for each tooth according to the pressure ratio across it. Regarding the carry-over factor a different formulation from Vermes one is assumed by including the effect of the number of teeth and neglecting the impact of tooth width:

$$\mu = \sqrt{\frac{N}{N \cdot (1-\alpha) + \alpha}} \quad \text{with} \quad \alpha = 1 - \frac{1}{\left(1 + 16.6 \cdot \frac{c}{t}\right)^2} \tag{8}$$

Other indirect methods based on a very similar equation can be found in the literature, such as the one proposed by Eser et al. [18] or the one of Scharrer et al. [19]. Since they only slightly differ from the Neumann model, they are not included in the present study without any lack of completeness and generality.

2.2.2. Kurohashi Equation

Kurohashi model is reported in [20]. He assumed the same flow coefficient as Neumann given by Chaplygin formula. However, he proposed a modified carry-over factor by introducing a different formulation for the first tooth and the subsequent ones. This allows us to account for the significantly different aerodynamics between the flow field approaching the first and the following constrictions. Kurohashi's carry-over factor is defined as:

$$\mu_i = \begin{cases} \sqrt{\frac{1}{1-\alpha_i+\alpha_i^2}} & \text{for} \quad i = 1 \\ \sqrt{\frac{1}{1-2\alpha_i+\alpha_i^2}} & \text{for} \quad i > 1 \end{cases} \quad \text{with} \quad \alpha_i = \frac{\frac{c}{t}}{\frac{c}{t} \cdot K_i + \tan 6^\circ} \tag{9}$$

It can be noted that Kurohashi included the dependency of carry-over on geometrical features and on the jet expansion angle inside the cavity as Hodkinson did.

2.2.3. Morrison Equation

Morrison developed his model in [21]. All the direct methods reported so far assumed that the flow coefficient of the first tooth of a multiple-tooth labyrinth seals is the same as that of a single sharp-edged annular orifice. Actually, a single value for the whole labyrinth seal is considered but the flow coefficient of the first tooth may differ from that of the subsequent ones since the velocity profile at the inlet of the teeth following a cavity is not the same as that approaching the first tooth. The indirect models described so far try to capture this features by means of Chaplygin formula, hence introducing the effect of the tooth-by-tooth pressure ratio. However, Morrison rejected this method and defined a "discharge coefficient" in order to describe the total losses that occur as the flow passes through the tip clearance and inside the cavity. Thus, the traditional product between the flow coefficient and the carry-over factor in Equation (1) is replaced by the discharge coefficient given as a function of the carry-over factor. In particular, a different equation is provided for both the first tooth and the following ones, and the dependency on the pressure ratio is neglected. Hence, the discharge coefficient of the first tooth is given as a function of the flow Reynolds number and of the tip width-to-clearance ratio, while the contribution of the carry-over factor is added for the subsequent teeth. The carry-over does not depend on the number of teeth but on the c/t and w/s ratios and on the flow Reynolds number.

Since the parameters definition by this model makes use of much longer equations than the previous approaches, they are not reported in this paper, for the sake of brevity. They can be easily found in the reference paper [21].

Table 1. Correlation summary.

	Flow Coefficient, K	Carry-Over Factor, μ	Other
Direct Methods			
Hodkinson [11]	Constant value [10]	$f(N, c/t)$	-
Vermes [2]	$f(Re, w/c)$ [12]	$f(t, w, c)$	-
Zimmermann [13]	$f(Re, PR, w/c)$	$f(N, c/t)$	-
Indirect Methods			
Neumann [16]	Chaplygin formula, $f(\beta_i, \gamma)$ [17]	$f(N, c/t)$	-
Kurohashi [20]	Chaplygin formula, $f(\beta_i, \gamma)$ [17]	$f(N_i, K, c/t)$	-
Morrison [21]	-	-	Discharge coefficient

2.3. Evaluation of Discharge Coefficient

The above-mentioned correlations provide different methods to predict both the carry-over factor and the flow coefficient. Both of those quantities allow us to properly describe the flow phenomena occurring inside a labyrinth cavity and hence, they give an estimation of the mass flow rate across the seal as a function of the available thermodynamic conditions. However, since the goal of the flow check tests is the characterization of the labyrinth seal, a non-dimensional discharge coefficient has been calculated as the ratio between the measured (or predicted) mass flow $\dot{m}$ and the ideal mass flow rate $\dot{m}_{is}$ coming from an isentropic expansion in a nozzle with the same cross-section area:

$$C_d = \frac{\dot{m}}{\dot{m}_{is}} \tag{10}$$

where the ideal mass flow rate was evaluated by means of the total temperature T_0 at the seal inlet, the overall pressure ratio PR across the seal calculated as p_0/p_N and the tip clearance area A:

$$\dot{m}_{is} = \frac{p_0 A}{\sqrt{T_0}} \cdot \sqrt{\frac{2\gamma}{R(\gamma-1)}\left[\left(\frac{1}{PR^*}\right)^{2/\gamma} - \left(\frac{1}{PR^*}\right)^{(\gamma+1)/\gamma}\right]} \tag{11}$$

The value of PR^* used in the equation is taken as the minimum between the actual PR across the seal and the critical one (≈1.893, since air is used), as it is considered that the flow can reach, at most, sonic conditions at the tip clearance section, where A is evaluated.

It should be noted that Equation (10) is the well-known definition of the discharge coefficient and it should not be confused with the "discharge coefficient" employed by Morrison inside his model (see Section 2.2.3).

3. Experimental Facility

The flow check tests were performed on both a straight-through and a stepped seal thanks to a dedicated experimental apparatus, developed in collaboration with Baker Hughes—Nuovo Pignone Tecnologie s.r.l. and installed in the Heat Transfer and Combustion Laboratory of the Department of Industrial Engineering of the University of Florence (DIEF).

A non-rotating test rig was designed, thus neglecting all the effects related to the rotation. These simplifications were justified by Waschka et al. [22] and by Paolillo et al. [8], who showed that, when axial velocity component of flow above the tooth's tip is higher than the circumferential velocity of rotor tip, the effect of rotation hardly affect the results. This condition was verified for the engine conditions that the present tests were aimed to simulate. Moreover, tests were carried out on linear test articles (i.e., representing a linearized slice of the full annular engine configuration), with a width (W) equal to around 200 times the clearance dimensions, thus minimizing border effects. The experimental campaign was carried out in scaled operating conditions, in order to improve the dimensional

accuracy, by increasing the test samples dimensions (a scale factor close to 3 was achieved), and to allow for an easier experimental approach with more manageable conditions. The test samples are representative of real labyrinth seals installed on BH engines. Each test sample is composed by four parts: the test article with the teeth, two lateral components, defining the resulting clearance size, and a top cover. All the components are made with stainless steel, by CNC or EDM (for the components with teeth) machining, and carefully assembled in order to reproduce the proper flow path and the right dimension of the clearance gap, as shown in Figure 3a,b.

The test rig is composed of a single fluid line (Figure 4). A compressor able of delivering air at a maximum pressure of 10 bar feeds the test rig. The air coming from the compressor is first dried, in order to prevent condensation during the expansion inside the test article. A pressure regulator provides a constant line-inlet pressure, while the mass flow rate (i.e., Reynolds number) through the rig is regulated by means of a chocked manual valve, upstream of the rig. Downstream of the second valve, a calibrated orifice flow meter is installed ($\pm 1.0\%$ accuracy). A separation plate divides the inlet plenum (i.e., test article feeding) and the discharge plenum. Since a uniform feeding of the test sample is required, the airflow enters the upper part of the inlet plenum radially, and then, a perforated plate is installed to damp the velocity components in non-axial direction. The test sample is located in the second chamber of the inlet plenum, installed on the separation plate. In order to provide a better understanding of the whole installation, a sketch of the test rig is provided in Figure 5. The discharge pressure can reach below-ambient conditions thanks to vacuum pumps, in order to maximize the achievable pressure ratio (PR) across the seal. This is regulated by a downstream manual valve and/or by the speed of the vacuum pumps. The upstream valve remains chocked throughout the whole operation, thus allowing to decouple Reynolds and PR regulation and to easily set the operating conditions. A safety valve is also installed upstream the test sample, in order to limit the maximum feeding pressure to the plenum. During the test rig operation, firstly, the shutter valve located upstream of the inlet plenum (see Figure 4) was regulated in order to set the desired Reynolds number (i.e., the mass flow rate across the seal). Then, the discharge pressure is controlled by means of the a ball valve (see "regulation valve" in Figure 4). A steady-state condition was reached after a time of 30 s and data were acquired for the next 10 s.

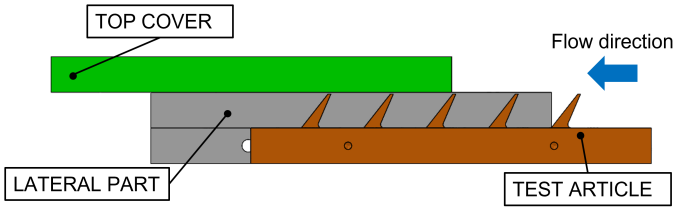

(**a**) Straight-through labyrinth seal.

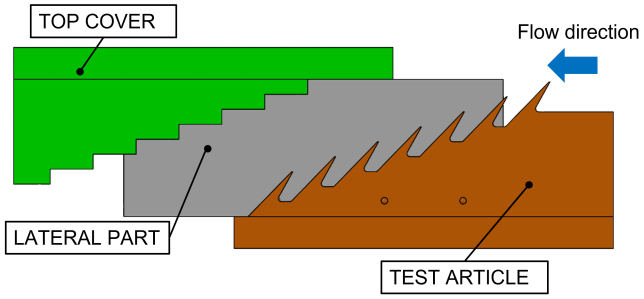

(**b**) Stepped labyrinth seal.

Figure 3. Assembly of a test sample representative of the tested labyrinth seal.

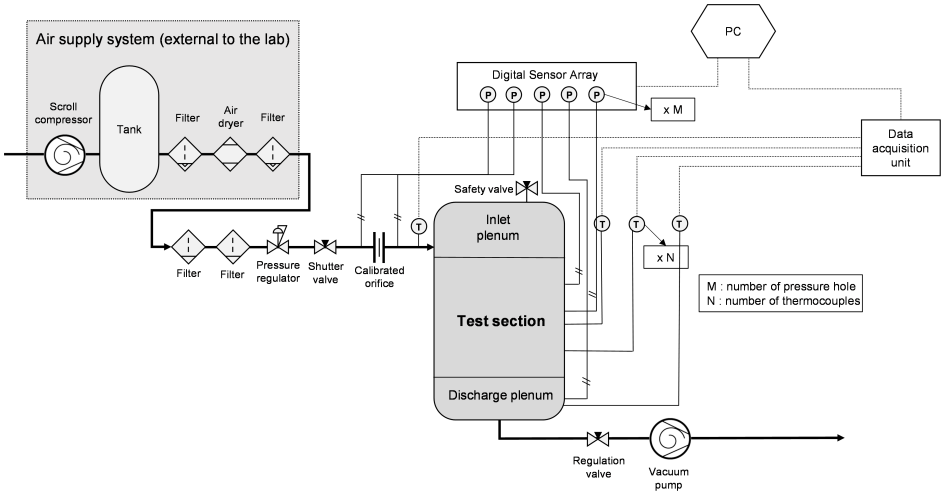

Figure 4. P&ID scheme of the test facility.

The pressures and the air temperatures are measured downstream of each tooth of the test articles in order to retrieve the pressure distribution across the seal and to evaluate the contribution of each tooth to the total pressure drop. Blind holes are also employed to measure the metal temperature in the proximity of the flow path. In addition, both the inlet plenum and the discharge plenum are equipped with pressure taps in order to check the global pressure ratio across the seal. All the temperatures are measured by T-type thermocouples ($\pm$0.5 K accuracy), while static pressures are retrieved by means of a ScaniValve DSA3217 ($\pm$52 Pa accuracy), with temperature-compensated piezo-resistive relative pressure sensors.

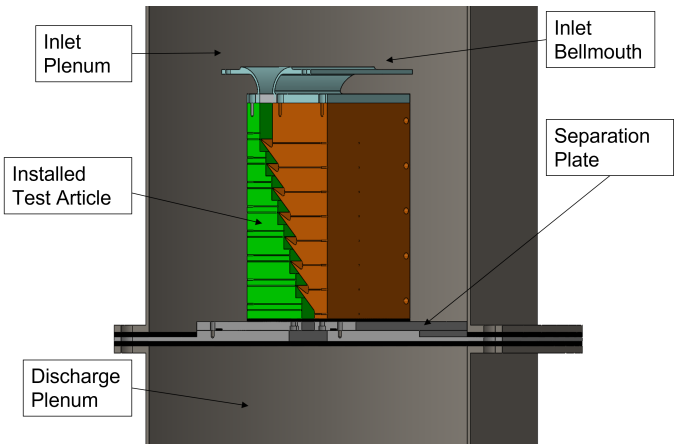

Figure 5. Sketch of the stepped test article installed inside the test rig.

The experimental campaign consisted of five test series with different values of clearance. For each test series, a double-regulation strategy was adopted. First of all, in order to provide a proper flow check curve around the nominal operating point of each seal, the conditions were changed by keeping the discharge pressure unaltered and varying the *PR*. In this way, a variation of both the Reynolds number and the pressure ratio occurred. Then, in order to evaluate the separated effect of the two parameters, a second regulation strategy was adopted by keeping the mass flow rate (i.e., the Reynolds number) unaltered to fixed values, and by varying the *PR* together with the rig-pressure level. It was therefore possible to achieve flow check curves with fixed Reynolds number (ranging between 60% and 140% of the nominal value) and varying PR. The whole test matrix is reported in Table 2.

Table 2. Test matrix.

	Straight-Through Seal	**Stepped Seal**
Nominal *Re* [-]	4000	4000
Nominal *PR* [-]	1.68	3.59
Discharge pressure at nominal conditions [PaA]	40,000	20,000
Tested *PR* range [-]	1.2–4.0	1.5–5.0
Tested *Re* range [-]	2400–5600	2400–5600

Investigated Geometries

The seal geometries analyzed in the present work are reported in Figure 3a,b. The stepped labyrinth has seven teeth, while the straight-through one has five teeth. Non-dimensional geometrical features are reported in Table 3. It is worth highlighting that the values of the clearance are very small, but they are characteristic of turbomachinery applications. Thus, for the smallest ones, the validity ranges of the above-mentioned correlations can be exceeded, in terms of clearance-to-pitch and tip width-to-clearance ratio. In addition, it should be noted that none of the available correlations take the inclination of teeth into account, but it is expected to affect the flow field inside the cavities and hence, both the flow coefficient and the carry-over factor.

Table 3. Test sample geometrical features.

	N	**c/w**	**c/t**	**c/h**	**s/c**	**α**	**β**
Straight-through seal	5	0.36–0.84	0.017–0.039	0.031–0.072	0.00	31.5°	15°
Stepped seal	7	1.12–2.44	0.029–0.063	0.042–0.091	5.46–11.8	37.5°	15°

4. Results

Before presenting the main outcomes of the above-mentioned correlative approaches, some results of the experimental campaign are shown. Tables 4 and 5 shows the complete test matrix of the second regulation strategy and the corresponding discharge coefficient for each test point; for a given pressure ratio value, the percentage difference is provided for each Reynolds number compared to the lowest one.

Table 4. Experimental discharge coefficient for each test Reynolds number and pressure ratio (straight-through labyrinth).

	$0.6Re_{nom}$	**$0.75Re_{nom}$**	**$0.9Re_{nom}$**	**$1.1Re_{nom}$**	**$1.25Re_{nom}$**	**$1.4Re_{nom}$**
$PR = 1.2$	0.409 (1)	0.414 (+1.17%)	0.421 (+2.91%)	0.424 (+3.72%)	0.426 (+4.33%)	0.427 (+4.33%)
$PR = 1.5$	0.433 (1)	0.440 (+1.66%)	0.448 (+3.57%)	0.452 (+4.40%)	0.453 (+4.73%)	0.452 (+4.40%)
PR_{nom}	0.443 (1)	0.454 (+2.40%)	0.461 (+4.02%)	0.466 (+4.99%)	0.467 (+5.39%)	0.467 (+5.29%)
$PR = 2.0$	0.466 (1)	0.476 (+2.11%)	0.485 (+4.11%)	0.490 (+5.23%)	0.492 (+5.64%)	0.493 (+5.81%)
$PR = 2.25$	0.476 (1)	0.487 (+2.18%)	0.497 (+4.29%)	0.502 (+5.43%)	0.503 (+5.68%)	0.505 (+6.11%)
$PR = 2.5$	0.483 (1)	0.492 (+1.97%)	0.504 (+4.27%)	0.509 (+5.42%)	0.512 (+6.01%)	0.513 (+6.25%)
$PR = 3.0$	0.491 (1)	0.500 (+1.81%)	0.510 (+3.97%)	0.515 (+4.89%)	0.518 (+5.54%)	0.519 (+5.72%)
$PR = 3.5$	0.495 (1)	0.505 (+2.05%)	0.512 (+3.56%)	0.518 (+4.69%)	0.520 (+5.13%)	0.521 (+5.32%)
$PR = 4.0$	0.496 (1)	0.505 (+1.83%)	0.516 (+4.09%)	0.519 (+4.79%)	0.521 (+5.13%)	0.523 (+5.48%)

Table 5. Experimental discharge coefficient for each test Reynolds number and pressure ratio (stepped labyrinth).

	$0.6Re_{nom}$	$0.75Re_{nom}$	$0.9Re_{nom}$	$1.1Re_{nom}$	$1.25Re_{nom}$	$1.4Re_{nom}$
$PR = 1.5$	0.272 (1)	0.272 (−0.07%)	0.272 (+0.00%)	0.271 (−0.42%)	0.273 (+0.59%)	0.275 (+1.12%)
$PR = 2.0$	0.303 (1)	0.300 (−1.02%)	0.299 (−1.22%)	0.302 (−0.39%)	0.303 (−0.03%)	0.304 (+0.19%)
$PR = 2.5$	0.317 (1)	0.317 (−0.03%)	0.317 (−0.03%)	0.321 (+1.06%)	0.321 (+1.18%)	0.321 (+1.23%)
$PR = 3.0$	0.326 (1)	0.327 (+0.30%)	0.327 (+0.43%)	0.327 (+0.35%)	0.329 (+0.96%)	0.330 (+1.20%)
PR_{nom}	0.331 (1)	0.332 (+0.03%)	0.332 (+0.28%)	0.334 (+0.72%)	0.335 (+1.00%)	0.335 (+1.11%)
$PR = 4.0$	0.334 (1)	0.334 (+0.19%)	0.335 (+0.43%)	0.336 (+0.76%)	0.337 (+1.10%)	0.338 (+1.22%)
$PR = 4.5$	0.335 (1)	0.336 (+0.25%)	0.338 (+0.78%)	0.339 (+0.91%)	0.339 (+1.05%)	0.340 (+1.28%)
$PR = 5.0$	0.337 (1)	0.339 (+0.59%)	0.338 (+0.25%)	0.339 (+0.65%)	0.340 (+0.79%)	0.341 (+1.26%)

The data of Tables 4 and 5 are plotted in Figure 6a and Figure 6b, respectively. They show the discharge coefficient as a function of the overall pressure ratio for different values of the tested Reynolds numbers for the straight-through and the stepped labyrinth seals, respectively, when the nominal value of the tip clearance gap is considered. It can be noticed that the higher the pressure ratio, the higher the C_d. However, as the pressure ratio increases, a well-established asymptotic trend is achieved. In addition, the Reynolds number has a very poor effect on the trends since the discharge coefficient slightly increases with the Reynolds number for a given value of pressure ratio. As shown by Figure 6 and by the percentage differences in the previous Tables, the values of the stepped seal overlap almost perfectly; for the straight-through seal, a 5% difference can be highlighted between the highest and the lowest Reynolds, hinting that, for this geometry, the asymptotic behavior is reached at a slightly higher Reynolds number. It can be speculated, even if not demonstrated by the present experimental research, that this is due to the higher momentum of the jet exiting from the constriction, resulting in higher carry-over effects (which are not present for the stepped seal).

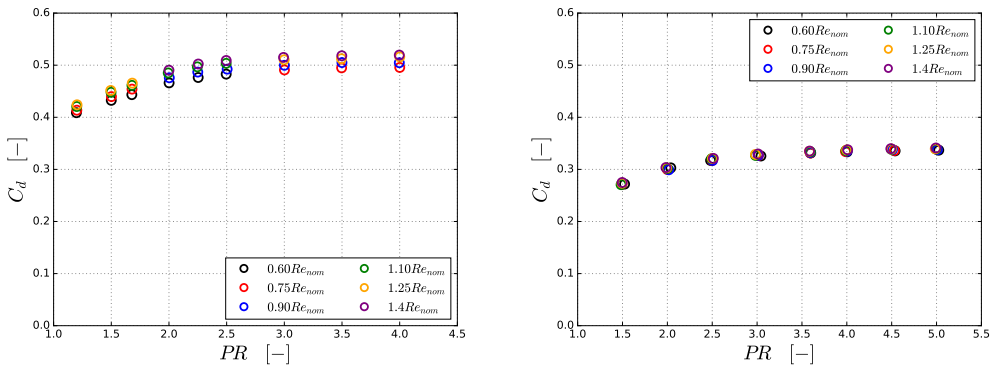

(**a**) Straight-through labyrinth seal. (**b**) Stepped labyrinth seal.

Figure 6. Discharge coefficient as a function of the overall pressure ratio for different values of the flow Reynolds number.

As a result, for both the tested labyrinth seals, the dependency of the discharge coefficient on the Reynolds number can be neglected and, in the following, most of the results will be presented at different flow Reynolds numbers without losing generality.

4.1. Straight-Through Labyrinth Comparison Results

In this section, the main results coming from the correlative models described in Section 2 are presented for the straight-through seal. Firstly, the estimated mass flow rate is compared with the measured one for the nominal value of the clearance. The estimated pressure distribution along the seal is shown for all the indirect models. Then, since one of the main contributions of this paper is to evaluate the relationship between the discharge coefficient and the clearance value, this trend is investigated for each correlation.

The experimental data shown in Figure 7a refer to the first regulation strategy explained in Section 3, hence both the Reynolds number and the overall pressure ratio change at each test point, as the discharge pressure is kept constant. Figure 7a shows the leakage mass flow rate as a function of the overall pressure ratio for the nominal clearance value. The expected increasing trend can be highlighted. The black solid line represents the experimental measurements, while the dashed lines depict the correlative methods. Both the direct and the indirect models are obviously able to reproduce the increasing trend and to provide an acceptable data matching, since the differences with respect to the experiments are, in general, quite limited. A deeper insight is provided by Figure 7b. It shows the percentage difference between the measured and estimated mass flow rate for each overall pressure ratio. All the correlation, except the Morrison one, underestimate the actual value of mass flow. In addition, all the indirect methods highlight an almost constant relative difference with varying PR. The direct methods, on the other hand, do not show the same behavior; Vermes and Hodkinson correlations provide a decreasing trend (i.e., increasing underestimation) for low PR, before settling to approximately constant values. The Zimmermann equation shows an increasing trend, as the underestimation reduces for increasing values of PR, and reaches an almost perfect matching (null relative difference with experiments) at the maximum tested PR. This is mainly due to the way the flow coefficient is modeled in those equations, since the same β term is included and the carry-over factor is fixed for a given clearance value, depending only on geometrical features. As stated in Section 2.1.1, Hodkinson suggested the employment of a constant K value, while the one provided by Vermes slightly depends on the Reynolds number (i.e., mass flow rate) and only a 4% increase is achieved when the Reynolds number is increased from the lowest to the highest value. A completely different situation shows up if the Zimmermann model is considered since the flow coefficient variation between the lowest and the highest Reynolds number is about 16%: the present benchmark shows that such a variation rate overestimates the actual one, at least for the tested seal geometry.

In order to provide a deeper comprehension of this dependence, Figure 8 shows the leakage mass flow percentage difference as a function of the overall pressure ratio when test points coming from the second regulation strategy (i.e., varying PR with constant Reynolds) are considered. The plot is referred to a flow Reynolds number of 5000 but similar results are found, and hence the same comments can be pointed out, if another Re number is taken. Although a slightly decreasing trend is achieved at the lowest PR values, a constant pattern is then achieved at higher pressure ratios for all the direct methods discussed so far: since a constant Reynolds results in a constant value of flow coefficient predicted by the considered direct methods, it is confirmed that the error variation evidenced in Figure 7b for Zimmermann approach is due to an incorrect modeling of the K-Re dependency, for the investigated geometry.

As stated above, the indirect models allow to retrieve the pressure distribution along the labyrinth, i.e., the pressure values downstream each tooth, knowing the inlet and the discharge pressures. Figure 9 shows the ratio p_n/p_N for two tested overall pressure ratios. It can be highlighted that, at the lower PR, the correlations can predict the experimental data with an almost-perfect fitting, while at the higher PR values, as the pressure variations are increased and the modeling is made more challenging, some differences arise, albeit quite limited ones. In particular, it should be noted that the steep pressure drop at the first tooth is not correctly reproduced by the Neumann model, since it does not distinguish between the different contribution of the first tooth and the following ones. On the other hand, both

Kurohashi and Morrison developed a dedicated formula to accurately characterize the influence of the flow field approaching the first tooth and the one developing inside each cavity and approaching the subsequent teeth. As a result, the pressure drop across the first tooth is properly reproduced, while an underestimation of the following teeth pressure is achieved.

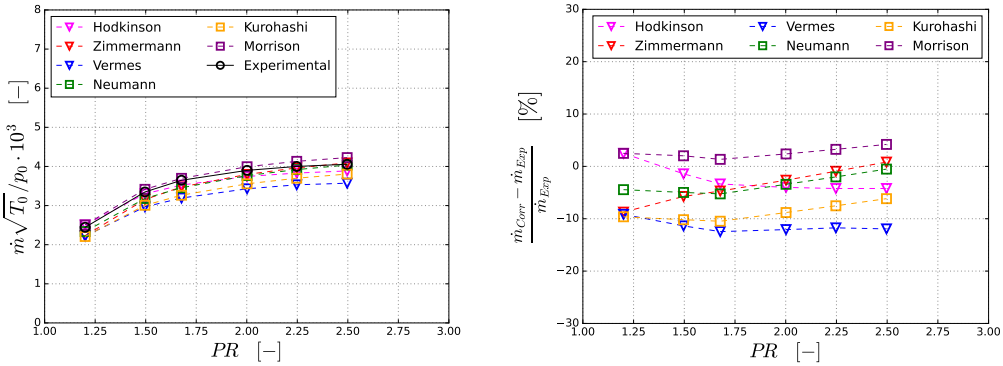

(**a**) (**b**)

Figure 7. Comparison between experimental mass flow data and calculated values coming from the correlations (straight-through labyrinth—nominal c value): (**a**) predicted/measured values and (**b**) relative differences

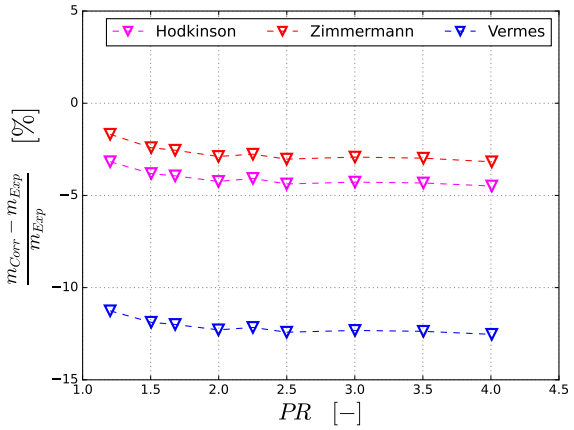

Figure 8. Percentage difference between experimental and analytical mass flow rates for tests at fixed Reynolds number value (straight-through labyrinth—$Re = 5000$—nominal c value).

Finally, the discharge coefficient is plotted for the nominal value of the pressure ratio as a function of the clearance-to-tip width ratio. Since the actual clearance value can change during the labyrinth life-cycle due to wear or thermal effects, it is key to evaluate the performance of the labyrinth for different value of the clearance gap size. Figure 10a shows the calculated discharge coefficients, while in Figure 10b, correlative results are scaled with experimental ones to produce relative differences. The black solid line in Figure 10a represents the experimental data: a decreasing trend can be highlighted. This means that, when increasing the clearance size, a reduction in carry-over factor or flow coefficient is achieved (or of both of them), but the precise reason can not be discerned from the available experimental results. The former (i.e., decrease in carry-over) can be achieved depending on the configuration of the jet exiting from one constriction; the latter (i.e., decrease in flow coefficient) can be generated by a limited variation of the actual area value A_j (see Figure 1), due to the flow field configuration inside the cavity and the resulting development of the vena contracta at the tooth tip: as the discharge coefficient values are calculated using the geometrical area A, which scales linearly with the clearance size, the resulting C_d trend would be decreasing. It must be pointed out that other studies [5] reported opposite results,

with increasing C_d trends as the clearance gap increases. As the main difference between those and the present study stays in the teeth inclination (straight for the referenced works and inclined backward for the present one), this is thought to be the main parameter determining the evidenced trend.

Looking back to Figure 10, only the Vermes correlation is able to reproduce the decreasing trend. It is worth reminding that all correlations return increasing carry-over factors, but Vermes is the only author that suggests the employment of a decreasing flow coefficient for increasing values of the clearance size, as reported in [2]. All the other models adopts an increasing flow coefficient for increasing clearance values and hence, they fail the prediction of the experimental trend. Since Vermes proposes increasing flow coefficient values for even higher gap sizes, this behavior is expected to reverse at some point (beyond tested values). The dependence of the predicted flow coefficient on Reynolds number, which is admitted by some correlations, is not expected to play a role in these results, since the same trend is achieved as the results at constant Reynolds (i.e., same Reynolds number for all clearance values) are considered (even if not shown in the paper). According to Figure 10b, the percentage values of all the correlations except Vermes range from -25% to $+25\%$. The shift between negative to positive values is related to the crossing of the experimental and analytical trends of Figure 10a. This variation is far more limited for the Vermes approach (from about -15 to -5%), thus showing, albeit with a certain offset, a more adequate modeling of the actual clearance behavior.

Overall, results point out that Vermes correlation, even if it was among the worst performing as far as the analysis was limited to the nominal clearance size (Figure 7), was revealed to be the only one able to accurately predict the seal behavior with changing clearance gap; significant mispredictions can be expected with the adoption of the other approaches, as the actual clearance size changes during the engine operability and lifetime.

As anticipated, it is also worth considering that all the employed equations were developed especially for straight-through seals with perfectly straight teeth, having a constant width moving from their hub to the tip. Thus, some geometrical features which defines the current seal, such as the α and δ angles, are not considered in those models, but they are expected to play a major role in the flow field and hence, in determining the effective value of the discharge coefficient.

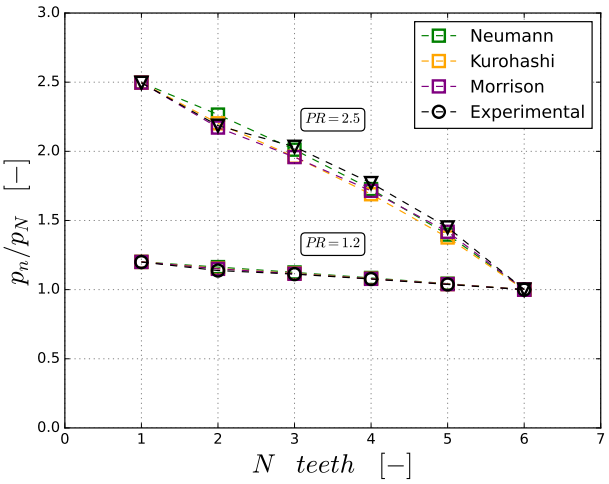

Figure 9. Pressure distribution across the straight-through labyrinth for two values ($PR = 1.2$ and $PR = 2.5$) of the overall pressure ratio (nominal c value).

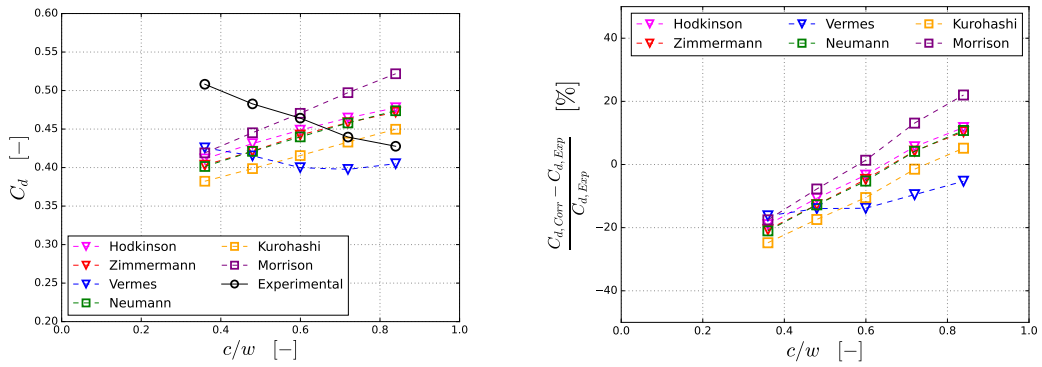

(**a**) (**b**)

Figure 10. Comparison between experimental and analytical discharge coefficient for increasing values of the clearance-to-tip width ratio (straight-through labyrinth—nominal *PR*): (**a**) predicted/measured values and (**b**) relative differences.

4.2. Stepped Labyrinth Comparison Results

In this section, the main results coming from the correlative analysis are presented for the stepped labyrinth seal. As already performed for the straight-through one, the estimated mass flow rate is compared with the measured one for the nominal value of the clearance. However, two different and complementary approaches are shown. Then, the pressure distribution coming from the indirect models is presented. Finally, the discharge coefficient as a function of the clearance size is discussed.

As already explained, the proposed analytical models were developed during the past decades specifically for straight-through labyrinths starting from the available empirical data. However, many authors recommend their application also for stepped seals as long as certain assumptions were made. In particular, Egli [10] and Vermes [2] stated that the carry-over coefficient should be neglected for stepped labyrinths. By making the step s sufficiently high, all the kinetic energy of the jet will be dissipated before the flow enters the next cavity. Hence, it was decided to eliminate the μ parameter from Equation (2). On the other hand, no indications are given for the indirect models. Thus, two different approaches have been employed; in the first case, the contribution of the carry-over factor μ_i was kept inside Equation (6) and, in the second case, it was removed. Results are shown in Figures 11 and 12. In particular, Figures 11a and 12a show that the mass flow rate increases for increasing values of the overall pressure ratio for the nominal clearance value. The black solid lines represent the experimental measurements, while the dashed lines depict the correlative methods. It is clear from Figure 11a that neglecting the carry-over factor in the direct models allows a proper experimental data fitting, whereas its employment inside Equation (6) determines up to a 60% overestimation of the actual mass flow (see Figure 11b) since the dissipation of kinetic energy is not correctly modeled. However, as shown by Figure 12a, a proper trend is restored whether the carry-over factor is neglected also for the indirect models. The percentage differences fall down to 16% (Figure 12b) in the worst case scenario represented by the Morrison correlation; it should be noted that w/c validity range is not fulfilled for the Morrison correlation and hence, the model could lose reliability. The correlative approaches mostly tend to overestimate the leakage mass flow, in a slightly decreasing extent, as the PR is increased; an increasing trend occurs only for the methods from Neumann and Kurohashi. After μ_i is removed from Equation (6), there is no difference between Neumann and Kurohashi models since they differs only by the carry-over factor formulation. Hence, both correlations gave the same results; this is clearly visible in Figure 12b, as Neumann and Kurohashi series perfectly overlap.

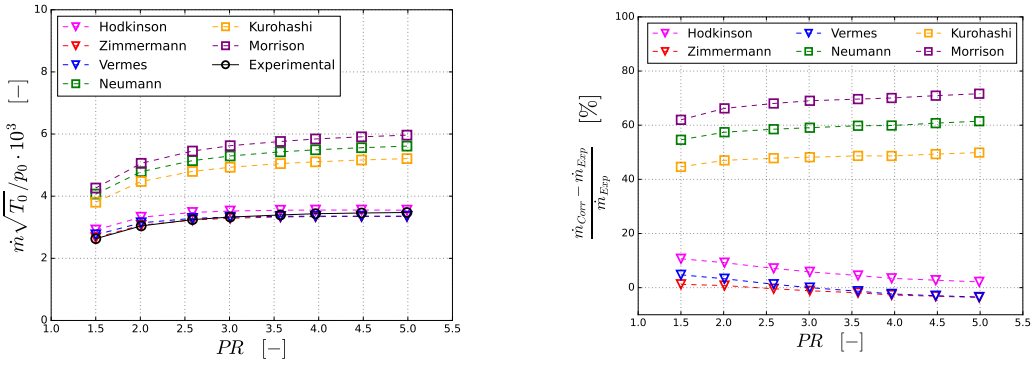

(**a**) (**b**)

Figure 11. Comparison between experimental mass flow data and calculated values coming from the correlations—carry-over factor is included in the indirect methods (stepped labyrinth—nominal c value): (**a**) predicted/measured values and (**b**) relative differences

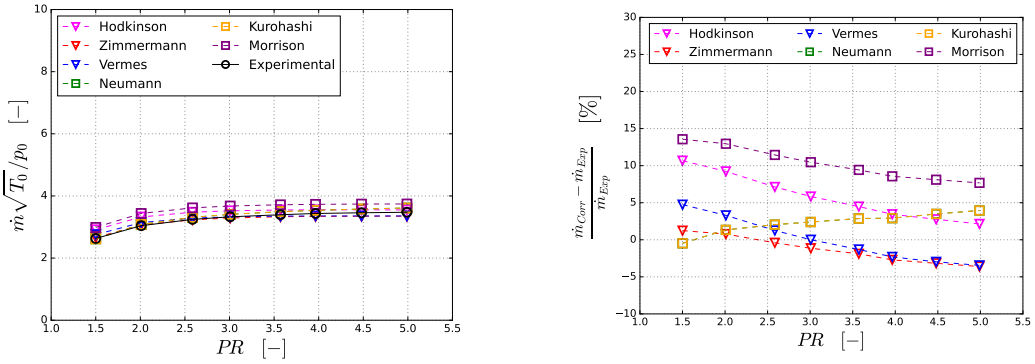

(**a**) (**b**)

Figure 12. Comparison between experimental mass flow data and calculated values coming from the correlations—carry-over factor is neglected in the indirect methods (stepped labyrinth—nominal c value): (**a**) predicted/measured values and (**b**) relative differences

Looking at the direct methods proposed in the present work, the percentage differences between experiments and correlations are plotted in Figures 12b and 13, for first and second regulation strategy, respectively. In both cases, all the analytical trends are monotonically decreasing as the PR increases. In particular, Hodkinson and Vermes lines have the same shape as, they both suggest a constant K value in the range of tested Reynolds number and clearance size. Further, Zimmermann does not provide a constant trend for a fixed Reynolds number even if he models the flow coefficient as a function of the PR [14]. Since the same decreasing trend is achieved regardless of the Reynolds value and variation rate, it can be stated that the mispredicted behavior stays in the dependence on the overall pressure ratio, through the β term in Equation (1) or its influence on the flow coefficient, for the stepped seals.

Figure 14 shows the pressure distribution across the stepped labyrinth for two investigated overall pressure ratios. As already shown for the straight-through labyrinth, at the lower PR, the indirect methods are able to match the experimental data. At the higher PR value, the Neumann and Kurohashi series collapse due to the carry-over removal but they underestimate the real values from 3% to 12% at the second and seventh tooth, respectively. On the other hand, Morrison slightly overestimates the actual trend but the percentage differences are below 10% for all the pressures. It can be seen that the pressure step at the first tooth disappeared and a smoother curve is obtained. This is mainly due to the removal of the carry-over factor from Equation (6) and it can be ascribed to the effect of the step height s on the kinetic energy. Its almost complete conversion into pressure energy inside

the seal cavity makes the flow field after each tooth more similar to that just before the first one.

Eventually, the discharge coefficient is plotted as a function of the clearance-to-tip width ratio in Figure 15, with the same approach used for the straight seal. A slightly decreasing trend can be highlighted in Figure 15a, even if the trend is not as smooth as the one found for the straight-through labyrinth. Looking at the series coming from the correlations, both Vermes and Zimmermann are able to capture the decreasing trend while an almost constant value is predicted by the others. Since carry-over effect have been shown to be negligible for stepped seals, this decreasing trend is surely due to the impact of flow coefficient in Equations (2) and (6). As stated in [13], Zimmermann suggested a flow coefficient extracted from available data derived from dedicated tests performed on these kinds of labyrinth. On the other hand, a decreasing value of the flow coefficient is prescribed for increasing clearance values, according to Vermes [2]. Despite the not perfectly smooth experimental trend, Vermes correlation is the one that provides the best prediction of the overall C_d reduction rate, as the clearance size is increased. Figure 15b highlights that for all the undertaken methods the values ranges from −10% to +10%. Hodkinson and Kurohashi models show, overall, the lowest relative differences, as their constant predicted value can be read as a mean value of the experimental discharge coefficients.

To conclude, it is worth reminding that the proposed correlations do not include all the geometrical parameters of the seals. For instance, the height of the step s is supposed to be the key in promoting the dissipation of kinetic energy and determining the flow path inside the cavity. In addition, validity ranges are not fulfilled for the Morrison correlation both for the straight-through and the stepped seal, since the w/c ratio exceeds the prescribed values.

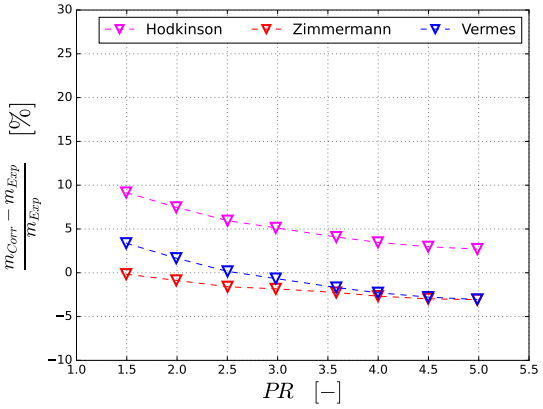

Figure 13. Percentage difference between experimental and analytical discharge coefficient values for tests at fixed Reynolds number value (stepped labyrinth—$Re = 5000$—nominal c value).

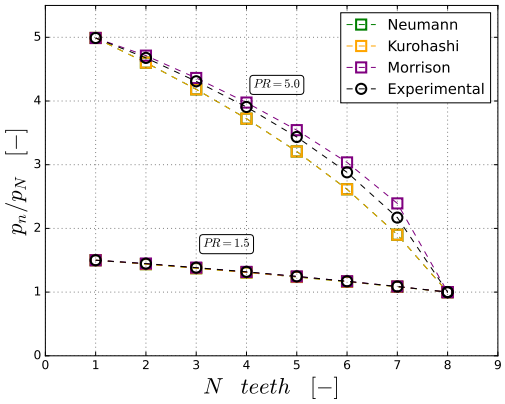

Figure 14. Pressure distribution across the stepped labyrinth for two values ($PR = 1.5$ and $PR = 5.0$) of the overall pressure ratio (nominal c value).

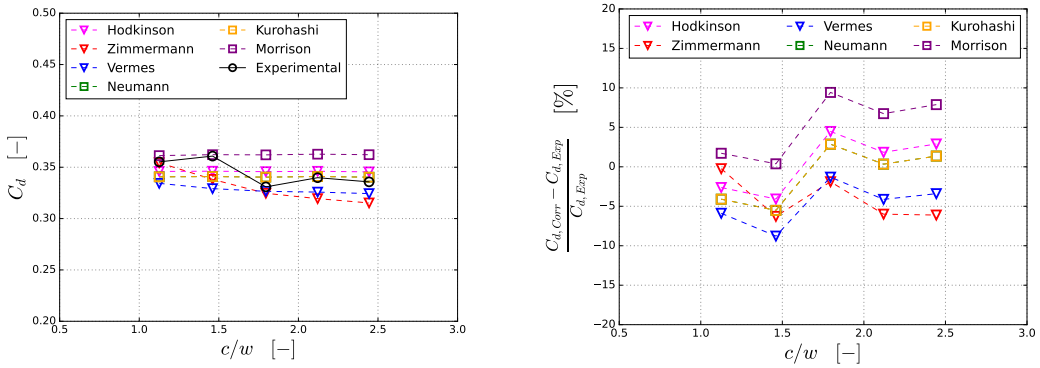

(**a**) (**b**)

Figure 15. Comparison between experimental and analytical discharge coefficient for increasing values of the clearance-to-tip width ratio (stepped labyrinth—nominal *PR*): (**a**) predicted/measured values and (**b**) relative differences.

5. Conclusions

In order to verify and compare the reliability of state-of-the-art correlations for the prediction of leakage mass flow through a labyrinth seal, the results of a wide experimental campaign performed on both a straight-through and a stepped seal are compared to the predictions estimated through the most-known analytical approaches. In general, in the evaluation of the results, attention was paid, not only to investigate the correlations that provided the closest match to the experimental findings, but especially to highlight the precision in the modeling of the impact of different parameters through the evaluation of the error trends.

A dedicated test rig was used to characterize the seals behavior by varying the overall pressure ratio and the Reynolds number independently from each other; this allowed us to acquire test points by changing *PR* and *Re* simultaneously (by keeping the outlet pressure unaltered and varying the inlet one) and by changing PR with constant Reynolds (by varying both inlet and outlet pressure). In this way, it was possible to evaluate the accuracy of the considered correlative approaches and highlighting their limitation in modeling the impact of these two parameters on the resulting leakage mass flow rate.

In general, the following indications could be provided:

- For the straight-through seal and nominal clearance size, the impact of the Reynolds number was overestimated by the Zimmermann correlation, whereas a better modeling was achieved through Vermes and Hodkinson ones.
- For the stepped seal, the need for improvement in the modeling of the impact of the overall pressure ratio was evidenced, for all approaches. Carry-over effects must be also neglected to achieve a proper prediction.
- Concerning the evaluated pressure distribution across the seal, thanks to the indirect models, the possibility to distinguish between the behavior of the first and the following constrictions is mandatory to achieve a reliable prediction for the straight-through seal.
- Concerning different clearance sizes, for the straight-through seal, Morrison correlation provided the best matching for the straight-through seal at the nominal clearance size, with errors within 5% in the tested *Re*-*PR* range; on the other hand, errors reached ±20%, if all clearance values were considered. Vermes correlation, while being among the worst-performing for the nominal clearance size (errors around 10%), is the only one that can correctly predict the performance trend induced by the clearance variation.
- Similar considerations could be made for the stepped seal, with more limited variations and overall errors.

- Overall, Vermes correlation has been revealed to be the best performing. It provides the more accurate modeling of different aspects, thus returning correct trends, despite a certain offset, with respect to experimental findings.
- The adoption of a correlation able to correctly predict the behavior of the seal at different clearance sizes is crucial since its value is generally known with a limited accuracy during the engine operation and lifetime. The benchmark of a certain correlative approach for different values of clearance sizes is, therefore, evidenced as a mandatory step.

Author Contributions: Conceptualization, T.B., A.P., B.F. and L.W.; methodology, T.B., A.P. and B.F.; software, N.C., T.B. and A.P.; validation, N.C., T.B., A.P. and L.W.; formal analysis, N.C., T.B. and A.P.; investigation, N.C., T.B. and A.P.; resources, N.C., T.B., A.P. and L.W.; data curation, N.C. and T.B.; writing—original draft preparation, N.C. and T.B.; writing—review and editing, N.C. and T.B.; supervision, B.F.; project administration, L.W.; funding acquisition, B.F. and L.W. All authors have read and agreed to the published version of the manuscript.

Funding: This research was co-funded by Baker Hughes.

Data Availability Statement: Not applicable.

Acknowledgments: Baker Hughes is thankfully acknowledged for the possibility of publishing the results and for partially funding the research. The publication was made with the contribution of the researcher Tommaso Bacci with a research contract co-funded by the European Union—PON Research and Innovation 2014–2020 in accordance with Article 24, paragraph 3a), of Law No. 240 of 30 December 2010, as amended, and Ministerial Decree No. 1062 of 10 August 2021.

Conflicts of Interest: The authors declare no conflict of interest.

Nomenclature

Latin Letters		
A	geometrical area	[mm^2]
A_j	actual flow area	[mm^2]
A_m	vena contracta area	[mm^2]
c	clearance height	[mm]
C_d	discharge coefficient	[-]
h	tooth height	[mm]
K	flow coefficient	[-]
$\dot{m}$	leakage mass flow rate	[g/s]
N	number of teeth	[-]
p	pressure	[Pa]
PR	overall pressure ratio	[-]
R	gas constant	[J kg^{-1} K^{-1}]
Re	Reynolds number	[-]
s	step height	[mm]
t	tooth pitch	[mm]
T	temperature	[K]
w	tip tooth width	[mm]
Greek Letters		
α	geometrical factor	[-]
β	pressure factor	[-]
γ	air specific heat ratio	[-]
δ	seal angle	[°]
ϕ	tooth-by-tooth pressure ratio factor	[-]
μ	carry-over factor	[-]
θ	seal angle	[-]
Acronyms		
BH	Baker Hughes	
CNC	Computerized Numerical Control	
EDM	Electrical Discharge Machining	

References

1. Denecke, J.; Schramm, V.; Kim, S.; Wittig, S. Influence of rub-grooves on labyrinth seal leakage. *J. Turbomach.* **2003**, *125*, 387–393. [CrossRef]
2. Vermes, G. A fluid mechanics approach to the labyrinth seal leakage problem. *J. Eng. Power* **1961**, *83*, 161–169. [CrossRef]
3. Willenborg, K.; Kim, S.; Wittig, S. Effects of Reynolds number and pressure ratio on leakage loss and heat transfer in a stepped labyrinth seal. *J. Turbomach.* **2001**, *123*, 815–822. [CrossRef]
4. Micio, M.; Facchini, B.; Innocenti, L.; Simonetti, F. Experimental investigation on leakage loss and heat transfer in a straight through labyrinth seal. In Proceedings of the Turbo Expo: Power for Land, Sea, and Air, Vancouver, BC, Canada, 6–10 June 2011; Volume 54655, pp. 967–979.
5. Kim, T.S.; Cha, K.S. Comparative analysis of the influence of labyrinth seal configuration on leakage behavior. *J. Mech. Sci. Technol.* **2009**, *23*, 2830–2838. [CrossRef]
6. Szymanski, A.; Dykas, S.; Wróblewski, W.; Majkut, M.; Strozik, M. Experimental and numerical study on the performance of the smooth-land labyrinth seal. In Proceedings of the Journal of Physics: Conference Series, Słok near Bełchatów, Poland, 1–14 September 2016; Volume 760, p. 012033.
7. Gamal, A.J.; Vance, J.M. Labyrinth seal leakage tests: Tooth profile, tooth thickness, and eccentricity effects. *J. Eng. Gas Turbines Power* **2008**, *130*, 012510. [CrossRef]
8. Paolillo, R.; Moore, S.; Cloud, D.; Glahn, J.A. Impact of rotational speed on the discharge characteristic of stepped labyrinth seals. In Proceedings of the Turbo Expo: Power for Land, Sea, and Air, Montreal, QC, Canada, 14–17 May 2007; Volume 47934, pp. 1291–1298.
9. Denecke, J.; Dullenkopf, K.; Wittig, S.; Bauer, H.J. Experimental investigation of the total temperature increase and swirl development in rotating labyrinth seals. In Proceedings of the Turbo Expo: Power for Land, Sea, and Air, Reno, NV, USA, 6–9 June 2005; Volume 47268, pp. 1161–1171.
10. Egli, A. The leakage of steam through labyrinth seals. *Trans. Am. Soc. Mech. Eng.* **1935**, *57*, 115–122. [CrossRef]
11. Hodkinson, B. Estimation of the Leakage through a Labyrinth Gland. *Proc. Inst. Mech. Eng.* **1939**, *141*, 283–288. [CrossRef]
12. Bell, K.; Bergelin, O. Flow through annular orifices. *Trans. Am. Soc. Mech. Eng.* **1957**, *79*, 593–601. [CrossRef]
13. Zimmermann, H.; Wolff, K. Air system correlations: Part 1—Labyrinth seals. In Proceedings of the Turbo Expo: Power for Land, Sea, and Air, Stockholm, Sweden, 2–5 June 1998; Volume 78651, p. V004T09A048.
14. Kearton, W.; Keh, T. Leakage of air through labyrinth glands of staggered type. *Proc. Inst. Mech. Eng.* **1952**, *166*, 180–195. [CrossRef]
15. Vennard, J.K. *Elementary Fluid Mechanics*; John Wiley & Sons: Hoboken, NJ, USA, 1995.
16. Childs, D. *Turbomachinery Rotordynamics: Phenomena, Modeling, and Analysis*; John Wiley & Sons: Hoboken, NJ, USA, 1993.
17. Iodide, S.; Jodate, S. *Theory of Jets in Ideal Fluids*; Gurevich, M.I., Translator; Pergamon Press Ltd.: Oxford, UK, 1966 .
18. Eser, D.; Kazakia, J.Y. Air flow in cavities of labyrinth seals. *Int. J. Eng. Sci.* **1995**, *33*, 2309–2326. [CrossRef]
19. Scharrer, J.K. Theory versus experiment for the rotordynamic coefficients of labyrinth gas seals: Part I—A two control volume model *J. Vib. Acoust. Stress Reliab.* **1988**, *110*, 270–280. [CrossRef]
20. Kurohashi, M.; Inoue, Y.; Abe, T.; Fujikawa, T. Spring and damping coefficients of the labyrinth seals. In Proceedings of the 2nd International Conference. Vibrations in Rotating Machinery, Cambridge, UK, 1–4 September 1980; pp. 215–222.
21. Suryanarayanan, S.; Morrison, G.L. Labyrinth seal discharge coefficient for rectangular cavities. In Proceedings of the Fluids Engineering Division Summer Meeting, Vail, CO, USA, 2–6 August 2009; Volume 43734, pp. 99–114.
22. Waschka, W.; Wittig, S.; Scherer, T.; Kim, S. Leakage Loss and Heat Transfer in High-Speed Rotating Labyrinth Seals: An Experimental Verification of Numerical Codes. In Proceedings of the Yokohama International Gas Turbine Congress (IGTC), Yokohama, Japan, 27 October–1 November 1 1991; Volume 2, S. II239-247.